

Hypoxia in cervical cancer: from biology to imaging

Heidi Lyng¹ · Eirik Malinen^{2,3}

Received: 22 May 2017 / Accepted: 24 June 2017 / Published online: 10 July 2017
© The Author(s) 2017. This article is an open access publication

Abstract

Purpose Hypoxia imaging may improve identification of cervical cancer patients at risk of treatment failure and be utilized in treatment planning and monitoring, but its clinical potential is far from fully realized. Here, we briefly describe the biology of hypoxia in cervix tumors of relevance for imaging, and evaluate positron emission tomography (PET) and magnetic resonance imaging (MRI) techniques that have shown promise for assessing hypoxia in a clinical setting. We further discuss emerging imaging approaches, and how imaging can play a role in future treatment strategies to target hypoxia.

Methods We performed a PubMed literature search, using keywords related to imaging and hypoxia in cervical cancer, with a particular emphasis on studies correlating imaging with other hypoxia measures and treatment outcome.

Results Only a few and rather small studies have utilized PET with tracers specific for hypoxia, and no firm conclusions regarding preferred tracer or clinical potential can be drawn so far. Most studies address indirect hypoxia imaging with dynamic contrast-enhanced techniques. Strong evidences for a role of these techniques in hypoxia imaging have been presented. Pre-treatment images have shown significant association to outcome in several studies,

and images acquired during fractionated radiotherapy may further improve risk stratification. Multiparametric MRI and multimodality PET/MRI enable combined imaging of factors of relevance for tumor hypoxia and warrant further investigation.

Conclusions Several imaging approaches have shown promise for hypoxia imaging in cervical cancer. Evaluation in large clinical trials is required to decide upon the optimal modality and approach.

Keywords Cervical cancer · Imaging · Hypoxia · Positron emission tomography · Magnetic resonance imaging · Treatment outcome

Introduction

Tumor hypoxia is an adverse factor in cervical cancer and associated with poor outcome regardless of treatment modality [1–4]. Therapeutic strategies to handle hypoxia are, therefore, highly needed, especially for locally advanced stages, where radiotherapy, often combined with cisplatin, is the main treatment option. Although local recurrence occurs in only about 10% of the cases, more than 30% experience distant relapse [5]. For stage III–IVa disease, the numbers are even higher. During radiotherapy, high radiation doses are applied to increase the likelihood of tumor control. Thus, many patients face severe damage to critical organs in the pelvis after therapy, including fistulas and rectal bleeding [5]. Strategies for modifying tumor hypoxia by normobaric or hyperbaric oxygen, or by use of nitroimidazole compounds as radiosensitizer, have been shown to improve radiotherapy outcome [6]. Modern approaches, combining radiation with molecular targeted drugs or escalating the radiation dose to hypoxic tumor

✉ Heidi Lyng
heidi.lyng@rr-research.no

¹ Department of Radiation Biology, Institute for Cancer Research, Norwegian Radium Hospital, Oslo University Hospital, Oslo, Norway

² Department of Medical Physics, Norwegian Radium Hospital, Oslo University Hospital, Oslo, Norway

³ Department of Physics, University of Oslo, Oslo, Norway

regions, are on the agenda [7, 8], but such approaches strongly rely on robust hypoxia biomarkers. Medical imaging could allow for visualization of hypoxia within the entire tumor prior to and during therapy. In this respect, imaging is superior to the traditional invasive biomarker assays based on needle electrodes or tissue sampling.

Imaging is the cornerstone in diagnosis, radiotherapy planning, and treatment monitoring of cervical cancer [9]. Multimodality imaging with T2-weighted magnetic resonance imaging (MRI) and computed tomography (CT) is current state of the art for defining target volumes and calculating radiation doses delivered to the patient both for the external radiation therapy and for the brachytherapy. Fluorine 18-fluorodeoxyglucose (18F-FDG) positron emission tomography/computed tomography (PET/CT) may aid detection of pathological lymph nodes, and is becoming increasingly common for defining nodal targets. Functional MRI, including dynamic contrast-enhanced (DCE) and diffusion-weighted (DW) MRI, may improve target definition and is part of the standard imaging protocol at many institutions. In addition, recent technological developments, such as the PET/MRI hybrid scanners and MRI linear accelerator, will facilitate more advanced use of imaging in years to come. The first experience with PET/MRI in cervical cancer has shown improved integration of anatomical and functional tumor characteristics in MR and PET images and more reliable target definition as compared with PET/CT [10].

To date, imaging has almost exclusively been used for assessing anatomical features, such as tumor size, stage, and spread of the disease. There are emerging data showing that PET and MRI have a huge potential in visualization of hypoxia in cervix tumors. Here, we review current biological knowledge of hypoxia and hypoxia markers of relevance for imaging. We further discuss imaging techniques that have shown promise in a clinical setting to evaluate hypoxia and predict and monitor treatment outcome in cervical cancer, and address how these may play a role in new strategies to improve treatment outcome.

The biology of hypoxia

Tumor oxygen levels

Earlier studies assessing oxygen tension (pO_2) in tumors by use of the Eppendorf electrodes have clearly demonstrated that hypoxia is a common feature of cervical cancer. Cohort-based median pO_2 levels ranging from 2 mmHg (0.3% O_2) to 14 mmHg (1.8% O_2), as measured before the start of treatment, have been reported [1, 3, 11–13]. There are, however, considerable differences between individual tumors, and hypoxic fraction, in

terms of pO_2 readings below 5 mmHg (0.7% O_2), can differ from 0 and up to 100%. A large pre-treatment hypoxic volume has been associated with the presence of lymph node metastases at diagnosis and poor overall or disease free survival [1–4]. Similar associations have been reported for locoregional control, but the data are less consistent probably due to few relapses in small patient cohorts. The significance is generally retained in multivariate analysis with clinical markers such as tumor stage and size [1, 2, 4]. Assessment of hypoxia status would, therefore, add valuable information to the traditional diagnostics in treatment planning.

Although some tumors are more hypoxic than others, a large intratumor heterogeneity in the oxygen levels exists, and sampling from several regions is required to achieve reliable hypoxia estimates that can be compared across patients [14]. Imaging is particularly appealing in this respect by providing information from the entire tumor. A challenge is, however, the small size of the hypoxic regions, which can be below the spatial resolution of medical images. Hence, pO_2 levels ranging from 1 to 20 mmHg (0.1–2.6% O_2) over a distance of less than 1 mm have been measured [15], and even smaller hypoxic patches of a couple of cell diameters have been detected with immunohistochemistry, using the hypoxia marker pimonidazole [16].

Tumor hypoxia is not static, but evolves and diminishes in a dynamic process depending on tumor growth, neo-angiogenesis, and treatment [17]. Thus, temporal fluctuation in pO_2 over short time periods of less than 1 h has been detected in cervical cancer xenografts [18]. In an orthotopic cervical cancer mouse model, exposing the mice to varying O_2 concentrations in cycles during tumor growth was shown to enhance the capability of tumor cells to metastasize to local lymph nodes [19]. This suggests that O_2 fluctuations could be of clinical relevance. There is a lack of information on cycling hypoxia in human tumors, and imaging could facilitate such investigations by repetitive non-invasive measurements.

Changes in tumor hypoxia have been measured during fractionated radiotherapy [13, 20–22]. In a study comparing pO_2 data before treatment and after 10 Gy of radiation, increased oxygenation was primarily found in the most oxygenated tumors, while the hypoxic tumors showed no change or a decrease [22]. This observation was attributed to more treatment-induced cell death and thereby probably a larger decrease in oxygen consumption in oxygenated tumors. The benefit of assessing hypoxia during therapy for outcome prediction is, however, not clear. Suzuki et al. [13] found a stronger association with locoregional control for pO_2 data measured after 2 weeks of external radiation, whereas pre-

treatment data performed better regardless of end-point in the study by Lyng et al. [4]. Tumor pO_2 measured after 26–52 Gy of external radiotherapy seems to be less useful [21].

Physiological and molecular hypoxia markers

Hypoxic tumors show specific physiological and molecular characteristics that can be visualized in medical images. Hypoxia occurs in poorly vascularized tumors, where the impaired oxygen supply is not capable of meeting the oxygen demand of the cells. Necrosis may develop under severe, long-lasting hypoxia, depending on the cells' ability to adapt to the oxygen and nutrient deprived conditions. Hence, a negative correlation has been found between fraction of necrosis and pO_2 in cervix tumors [23]. Several studies have addressed relationships between hypoxia and immunohistochemistry markers of oxygen supply and demand. Poorly vascularized tumors or tumor regions have shown low pO_2 [24, 25], and long intercapillary distance has been associated with locoregional relapse [25]. Vascular parameters may, therefore, serve as surrogate markers of hypoxia in cervix tumors before the start of treatment. However, associations with poor outcome have also been found in cases of high vascular density in hot spots, which may reflect high angiogenic activity not necessarily related to hypoxia [25, 26]. Treatment-induced cell death has been shown to be more important than vascular changes for reoxygenation during the early phase of radiotherapy, probably because only small changes in vascular density have occurred at this stage [22]. Tumor cellularity, therefore, seems to also influence the hypoxia status, most likely reflecting the oxygen demand.

Tumor cells adapt to the hypoxic environment partly through stabilization of hypoxia inducible factors HIF1A and EPAS1 (HIF2A), enhancing glycolytic activity to maintain ATP levels when mitochondrial activity has slowed down [27]. Proteins involved in glucose metabolism have been investigated as possible endogenous hypoxia markers in immunohistochemical studies. High expression of HIF1A and its target proteins glucose transporter SLC2A1 (GLUT1) and pH regulator CA9 has been found in cervix tumors that were identified as hypoxic by pimonidazole staining or electrode measurements [28–32]. However, the spatial overlap between protein expression and pimonidazole staining has been found to be poor in many tumors [28, 31]. Moreover, although significant association between clinical outcome and expression of HIF1A, SLC2A1, CA9, or the glycolytic enzymes HK2 and PFKM2 has been found both for early [33–35] and late stage disease [32, 36–43], conflicting results have been reported [29, 30, 41]. This can probably be explained, because HIF1A and its target genes may be regulated by

other factors than hypoxia, including reactive oxygen species (ROS), oncogenes, and metabolic stressors like lactate [27]. In addition, tumor cells rely in general on glycolysis rather than oxidative phosphorylation as energy source even in the presence of oxygen, a phenomenon termed the Warburg effect [27]. Rapidly proliferating cells can, therefore, have high glycolytic activity and express proteins involved in glucose metabolism regardless of hypoxia.

In addition to activation of the HIF pathway, hypoxia tolerance in tumors is also mediated by activation of the unfolded protein response (UPR) and inhibition of MTOR signaling [44]. In global gene expression studies, we found that both HIF targets and UPR genes were required to construct a robust hypoxia gene classifier that could be validated across two independent cervical cancer cohorts [45, 46]. The importance of UPR has been further emphasized by the observations that high expression of the UPR regulated protein LAMP3 promoted hypoxia-driven metastasis in an orthotopic cervical cancer model and was associated with hypoxia in patient tumors [47]. Increased understanding of the mechanisms underlying hypoxia-related aggressiveness will be important for development of new molecular imaging approaches.

Positron emission tomography (PET)

PET employing tracers specific for low oxygen concentrations in tissue is the most direct method for non-invasive 3D imaging of hypoxia [48–50]. In PET, tracers that carry a positron emitting radioisotope such as 18-Fluorine (18F) or 11-Carbon (11C) are intravenously administered. Following radioactive decay in the body, the positron may typically travel up to 1 mm before annihilating with an atomic electron. Subsequently, two high-energy photons are created in opposite directions at approximately 180 degrees from each other. The photon pair may be registered in the PET ring detector system as a so-called co-incidence, connecting a line of response through the patient and thus providing the basis for image formation. After acquiring sufficient number of co-incidences, which typically takes some minutes, a 3D image series are reconstructed most often alongside the CT image series provided by the PET/CT scanner.

Hypoxia PET tracers and uptake mechanisms

There are many properties that characterize a PET tracer's specificity to tumor hypoxia [48]. Of these are (1) retention in hypoxic but not normoxic tissue, (2) kinetics suitable for imaging, (3) appropriate lipo- and hydrophilicity for optimal cell membrane transport and clearance of non-bound tracer,

and (4) reflection of the return to normoxic conditions, if relevant. There are mainly two groups of hypoxia PET tracers: fluorine labeled nitroimidazoles and copper labeled diacetyl-*bis*(*N*4-methylthiosemicarbazone) (ATSM) analogues. Nitroimidazoles accumulate in cells by first a passive diffusion across the cell membranes. Thereafter, if hypoxia is present, the compound's nitro group undergoes chemical reduction in a multi-stage process mediated by nitroreductase enzymes. The intermediate products in this process are highly reactive and can bind to macromolecules in the cell, thereby fixating the reduced form of the tracer intracellularly. If oxygen is present, the reductive process is reversed and no reactive intermediates are formed [51]. Moreover, nitroimidazoles will not accumulate in necrotic tissues as active uptake is dependent on functioning nitroreductase enzymes [52].

Cu-ATSM belongs to the group of dithiosemicarbazones, which are chemically quite different, and thus show other pharmacokinetic properties compared to nitroimidazoles. Several positron emitting copper isotopes such as ^{60}Cu and ^{64}Cu may be used for complexing with ATSM [53]. Compared to 18F, e.g., ^{64}Cu has much longer half-life, which may facilitate wider distribution to centers not having PET cyclotron. In addition, the emitted positrons have shorter range, which may result in images with slightly higher resolution. However, Cu-ATSM uptake in hypoxic tissues is not completely understood [54]. The tracer has high membrane permeability, thereby allowing efficient diffusion. Intracellularly, it is believed that the Cu^{2+} part of the complex is irreversibly reduced to Cu^+ under hypoxia, possibly leading to the dissociation of Cu^+ -ATSM and trapping of the Cu^+ -ion. In the presence of oxygen, the reduction of Cu^{2+} may be counteracted by reoxidation, thus preventing dissociation of the complex and resulting in clearance from normoxic tissues [55].

Nitroimidazoles as hypoxia tracer

The most widespread nitroimidazole compound for hypoxia imaging is 18F-fluoromisonidazole (18F-FMISO) [52]. The tracer is highly lipophilic, ensuring high diffusion across cell membranes. However, this also causes very slow clearance of the tracer from normoxic tissue, making the tumor to blood ratio rather low. For optimal discrimination between hypoxic and normoxic tissue with 18F-FMISO PET, long intervals of typically 2 h between tracer injection and imaging are required [56]. Although the tracer has been extensively studied in a variety of cancers both pre-clinically and clinically, very little has been published on cervical cancer. In a recent study on 11 patients, pre-treatment 18F-FMISO PET indicated the presence of hypoxia in all tumors, where the extent of hypoxia was independent of tumor volume (Table 1) [57].

Neither associations between 18F-FMISO uptake and outcome nor relations to immunohistopathological or genetic markers were reported. The patients also underwent PET with 18F-FDG and multiparametric DCE- and DW-MRI, and the strongest correlation was found between maximum tumor uptake of 18F-FMISO and 18F-FDG.

Another relevant nitroimidazole for hypoxia PET is 18F-fluoroazomycin-araboside (18F-FAZA), which is less lipophilic and may display better uptake kinetics compared to 18F-FMISO [58]. 18F-FAZA uptake has shown to be highly correlated with pimonidazole staining in, among others, head and neck and cervical cancer xenografts [58]. In a study on 15 patients with cervical cancer, 18F-FAZA PET was done before, during and after external chemoradiotherapy (Table 1) [59]. 18F-FAZA uptake was visually evaluated, and only five patients showed marked tumor uptake. These patients had somewhat larger tumor and higher proportion of failures compared to 18F-FAZA-negative patients, although the patient cohort was too small to make firm conclusions. Moreover, four out the five patients still had marked 18F-FAZA uptake into the course of fractionated radiotherapy, but all patients were PET-negative after treatment.

Vercellino et al. [60] employed 18F-fluoroerythronitroimidazole (18F-FETNIM) PET prior to chemoradiotherapy of cervical cancer (Table 1). Sixteen patients underwent hypoxia PET alongside 18F-FDG PET and analysis of osteopontin blood serum levels. Osteopontin was included as it has been associated with tumor hypoxia in head and neck cancer [61]. 18F-FETNIM tumor uptake was difficult to discriminate from adjacent normal soft tissues, indicating rather low tumor specificity. In comparison, all tumors showed pronounced 18F-FDG uptake. No correlation was seen between 18F-FETNIM uptake and 18F-FDG uptake or osteopontin level. However, patients with high 18F-FETNIM uptake had significantly reduced outcome, although the choice of threshold, i.e., tumor to muscle ratio (*T/M*), for assigning patients to the high-uptake risk group was not elucidated.

Cu-ATSM as hypoxia tracer

The largest study conducted on hypoxia PET in cervical cancer to date is the multicenter trial on ^{60}Cu -ATSM initiated at Washington University (Table 1) [53, 62–64]. In this trial, ^{60}Cu -ATSM PET was conducted in dynamic mode, acquiring data from 0 to 60 or 30 to 60 min post injection. This rather short time interval between injection and imaging compared to nitroimidazole-based PET reflects the faster biokinetics of ^{60}Cu -ATSM. Results from 38 patients were reported in the final publication [62]. The published studies have shown that virtually all tumors have significant Cu-ATSM uptake, with a mean *T/M* of nearly 4.

Table 1 Selected hypoxia imaging studies in primary cervical cancer

Modality	Image parameter	References	No. of pts	Biological end-point	Clinical end-point
PET					
18F-FMISO	Uptake	[57]	11	18F-FDG PET (+)	Feasibility
18F-FAZA	Visual grading	[59]	15	ND	Survival (NS)
18F-FETNIM	<i>T/M</i>	[60]	16	Serum osteopontin (NS) 18F-FDG PET (NS)	Survival (÷)
60Cu-ATSM	<i>T/M</i>	[64]	15	CA9 expression (+)	Survival (÷)
		[62]	38	18F-FDG PET (NS)	Survival (÷)
MRI					
BOLD	Mean signal	[80]	30	ND	Tumor shrinkage (÷)
		[82]	65	ND	Short term treatment response (÷)
DCE-MRI	RSI	[86]	50	<i>pO</i> ₂ (+)	ND
		[87]	12 + 8	<i>pO</i> ₂ (+); cell density (÷)	ND
		[89]	37	Vessel density (+)	ND
		[96]	81	ND	Locoregional control (+); survival (+)
		[98]	13	ND	Tumor regression (+)
		[101]	98	ND	Locoregional control (+) Survival (+)
DCE-MRI	EF	[97]	85	ND	Survival (+)
DCE-MRI	<i>K</i> ^{trans}	[98]	13	ND	Tumor regression (+)
		[92]	78	ND	Locoregional control (+); survival (+)
DCE-MRI	<i>A</i> _{Brix}	[86]	50	<i>pO</i> ₂ (+)	Survival (+)
		[99]	57	Vessel density (+)	Survival (NS)
		[46]	78	Gene expression (÷, 46 pts)	Survival (+)
CT					
DCE-CT	BF	[88]	32	<i>pO</i> ₂ (+)	ND
DCE-CT	BV	[100]	93	ND	Tumor response (+)

Pts, patients; *T/M*, tumor to muscle ratio; RSI, relative signal increase; EF, enhancing fraction; BF, tumor blood flow; BV, blood volume; +, significant positive association with image parameter; ÷, significant negative association with image parameter; NS, not significant association with image parameter; ND, no association investigated

Patients with high *T/M* had significantly lower progression free survival compared to those with low *T/M*. Moreover, there was no correlation between the 60Cu-ATSM data and glucose uptake assessed by 18F-FDG PET. This is exemplified in Fig. 1, showing PET images of two patients with glucose-avid tumor being non-hypoxic and hypoxic, respectively. In a subgroup analysis ($n = 15$) comparing biopsy-based immunohistochemical markers and 60Cu-ATSM PET, patients with more hypoxic tumors had significantly higher CA9 expression compared to those with less hypoxia [64].

Although the 60Cu-ATSM work is the most extensive study on hypoxia PET in cervical cancer, it is challenging to evaluate the potential of this tracer in future trials. Judging from pre-clinical (non-cervix) data, intratumoral uptake patterns of 18F-FMISO and 64Cu-ATSM are similar, with slightly higher 64Cu-ATSM uptake, but the concordance varies between xenograft models [65–67]. Furthermore, carbogen breathing, known to cause elevation

of tumor oxygen levels, gave increased staining of a nitroimidazole-based immunomarker but no change in 64Cu-ATSM uptake [67]. In addition, Cu-ATSM uptake may be perfusion dependent [67], which was not the case for 18F-FMISO evaluated more than 2 h after tracer administration [52].

Fluorodeoxyglucose (FDG) as a potential surrogate hypoxia tracer

Cervix tumors are generally glucose avid, showing high signal intensity on 18F-FDG PET [68, 69]. For the last two decades, there has been an ongoing discussion on the potential use of 18F-FDG as a marker of tumor hypoxia [70–73]. Normal cells will indeed turn to glucose metabolism for ATP production when exposed to hypoxia (Pasteur effect). However, tumor cells, even at normoxic conditions, very often utilize glucose metabolism for ATP synthesis (Warburg effect). Thus, any increase in 18F-FDG

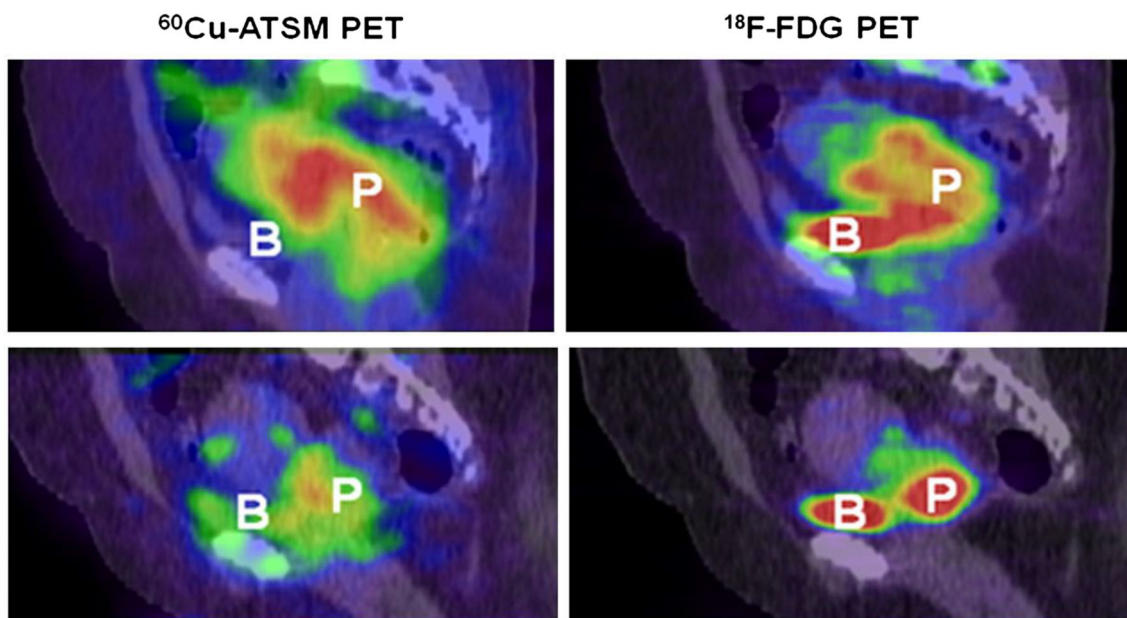


Fig. 1 Comparison of ^{60}Cu -ATSM and ^{18}F -FDG uptake in a hypoxic and normoxic cervix tumor. *Upper* hypoxic tumor. Sagittal ^{18}F -FDG PET/CT image (*right*) of pelvis, showing high ^{18}F -FDG uptake in tumor. Sagittal ^{60}Cu -ATSM PET image coregistered with CT image (*left*) at same level, also showing high tumor uptake of this tracer ($T/M = 4.5$). *Lower* normoxic tumor. Sagittal ^{18}F -FDG PET/CT image (*right*) of pelvis, showing high ^{18}F -FDG uptake in tumor.

Sagittal ^{60}Cu -ATSM PET image coregistered with CT image (*left*) at same level, showing only mildly increased tumor uptake of this tracer ($T/M = 3.0$). Note that there are different patterns of ^{18}F -FDG and ^{60}Cu -ATSM uptake in both tumors. *P* tumor, *B* bladder. This research was originally published in *JNM* [62]. © by the Society of Nuclear Medicine and Molecular Imaging, Inc

uptake due to hypoxia may well be obscured by that aerobic glycolysis already is activated. Moreover, common signatures of both hypoxia and aerobic glucose metabolism, such as GLUT1, HK2, and HIF1A expression, are often found to be elevated in cervix tumors [28, 74, 75]. Thus, depending on underlying activation of regulatory pathways, co-existence of hypoxia and aerobic glycolysis may be present in some tumors or tumor regions, but not in others. As virtually all cervix tumors are glucose avid, but not all are hypoxic, it is, therefore, not possible to pinpoint individual hypoxic tumors by ^{18}F -FDG PET with high accuracy. This is further exemplified in the literature on hypoxia PET tracers (Table 1), reporting varying degree of correlation between uptake of hypoxia tracer and ^{18}F -FDG.

BOLD—blood oxygenation level-dependent MRI and related techniques

In MRI, the paramagnetic properties of mainly tissue hydrogen are probed using a combination of an external magnetic field, magnetic field gradients, and frequency- and phase-encoded radiofrequency (RF) waves. Following an RF pulse with resonance frequency, the hydrogen nuclei experience relaxation through two principally different modes: T1- and T2 relaxation or longitudinal and

transverse relaxation, respectively. Relaxation rates are further influenced by other magnetic molecules in proximity, and MR image contrast arises from differences in hydrogen density and relaxation rates between tissues. In addition, inhomogeneities in the external magnetic field and local tissue magnetization will increase the transverse relaxation rate, leading to T2*-relaxation.

In blood vessels, hemoglobin (Hb) can be found as either oxyhemoglobin or deoxyhemoglobin (dHb), where oxygen-depleted tissues typically have high concentration of dHb. Deoxyhemoglobin is paramagnetic, and its presence will cause an increase in the T2*-relaxation rate $R2^*$ [76]. Thus, a decrease in blood oxygen saturation, indicating hypoxia, may be seen as a decrease in T2*-weighted image intensity or an increase in $R2^*$ image intensity. Therefore, sequences sensitive to blood saturation levels are denoted BOLD—blood oxygenation level-dependent MRI. BOLD MRI has shown significant association with tumor oxygen measures in both pre-clinical and clinical setting, although the literature is not fully consistent [76]. The feasibility of using BOLD in cervical cancer was investigated by Hallac et al. [77], where in total, nine patients were examined by two different MR acquisition techniques before and during oxygen breathing. Positive changes in BOLD signal intensity during breathing were found, albeit these changes were not highly tumor specific. A technique similar to BOLD, but which utilizes oxygen

dependent T1-relaxation, has been denoted TOLD—tissue oxygen-level-dependent MRI. Here, increase in T1 relaxation is caused by the presence of dissolved oxygen [76]. The technique was employed on two patients with cervical cancer and eight patients with other abdominal cancers during oxygen breathing [78]. A significant increase in signal intensity was found for both cervix tumors and six out of the remaining eight tumors, illustrating sensitivity of the method to oxygen modification. Furthermore, some resemblance was found between the TOLD images and perfusion images derived from DCE-MRI.

The approach of using oxygen breathing during BOLD or TOLD image acquisition is cumbersome and not suited for clinical routine. Utilizing the relaxation rate directly as hypoxia measure would, therefore, be more optimal, but there are many unresolved issues regarding absolute quantification [76, 79]. Nevertheless, BOLD was used in 30 cervical cancer patients to assess changes in tumor oxygenation after radiotherapy (Table 1) [80]. First, tumor $R2^*$ was markedly higher after therapy, indicating increased dHb levels and thereby possibly more hypoxia. This apparently unexpected observation was later confirmed in a second study from the same institution [81], and the authors argued that treatment-induced vascular damage could be a contributing factor. Second, high $R2^*$ was negatively associated with the percentage of tumor shrinkage [80], in line with the hypothesis that hypoxic tumors (with high $R2^*$) show poor response. This was further supported by a study on 65 patients [82], showing that non-responders had significantly higher $R2^*$ compared to responders. Moreover, in 30 patients with recurrent disease after surgery, hypoxic fraction derived from $R2^*$ mapping at the time of second line radiotherapy was significantly correlated with percentage of tumor shrinkage [83]. Thus, the body of literature on BOLD and related techniques in cervical cancer is more extensive and includes more patients than the literature on hypoxia PET tracers. Results from different studies are more or less consistent, warranting further clinical applications of this MR-based technique.

Dynamic contrast-enhanced (DCE) imaging

For DCE imaging with either MR or CT, a bolus of contrast agent is administered intravenously into the patient and transported via the blood stream to the tumor [76]. The low molecular weight contrast agents used in clinical routine move freely across the vessel walls in tumors and distribute in the extracellular space before being gradually washed out. For MRI, paramagnetic contrast agents, typically based on gadolinium, cause a signal intensity increase in T1-weighted images. Conversely, the contrast in CT

images is enhanced by iodinated contrast agents [84]. Rapid image acquisition is performed to track the contrast agent in tumor. Due to the highly permeable vessels in tumors, the uptake is perfusion limited, rather than limited by vessel permeability, and depends mainly on the blood flow, vascular density, and size of the extravascular, extracellular space [85]. For high molecular weight contrast agents, the tumor distribution is more dependent on vessel permeability. DCE imaging is unable to provide direct measures of tumor oxygenation. However, it is well documented that imaging with low molecular weight contrast agents can visualize tumor physiology related to hypoxia in cervical cancer.

Image parameters and relationship to hypoxia

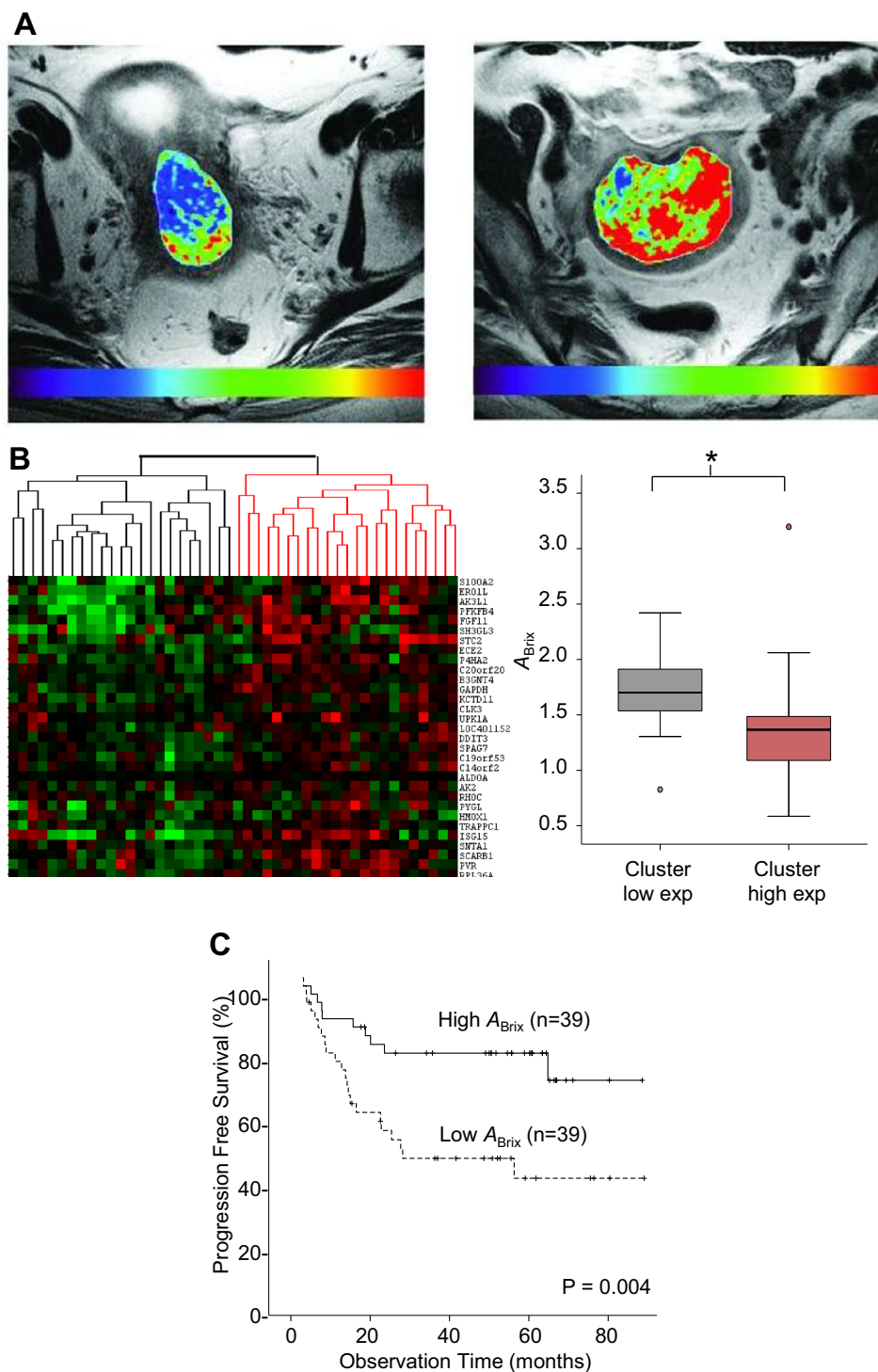
The easiest way of analyzing the transient uptake curves is by retrieving semi-quantitative measures such as the relative signal increase (RSI), the slope of the initial part of the curve, and the area under the curve over a certain time period (AUC). Such measures have been shown to correlate with pO_2 or hypoxic fraction in both MRI [86, 87] and CT [88] studies on cervical cancer (Table 1). Hence, hypoxic tumors or tumor regions typically display low signal enhancement in DCE images. Moreover, RSI has been shown to be associated with cell density [87] and vessel density [89] in tumor biopsies, and, therefore, probably reflects both oxygen demand and supply.

Quantitative image parameters, derived by fitting the uptake curves to pharmacokinetic models, provide more specific physiologic information. The most used parameters, K^{trans} from the Tofts model and A_{Brix} from the Brix model [90, 91], reflect blood perfusion and a combination of perfusion and the size of the extravascular, extracellular space, respectively [85]. In a study on 78 cervical cancer patients, the two parameters were found to be significantly correlated ($r = 0.56$) [92]. In addition, the v_e parameter from the Tofts model, which reflects the size of the extravascular, extracellular space, was found to be strongly associated with A_{Brix} ($r = 0.68$), but showed no relationship to K^{trans} [92]. Several studies have shown a relationship between K^{trans} or A_{Brix} and pO_2 in cervix tumors (Table 1) [86–88]. The A_{Brix} relationship was further supported by work at our institution by combined analysis of DCE-MR images and biopsy derived gene expression profiles (Table 1; Fig. 2) [46]. A significant correlation between A_{Brix} and hypoxia gene sets was demonstrated, and tumors with low A_{Brix} had upregulation of hypoxia responsive genes, including HIF1 targets and UPR genes.

Although CT is a widely available modality, only few studies have explored the potential of DCE-CT to visualize hypoxia in cervix tumors [88]. A strong correlation between the DCE-CT and -MRI parameters has been found

Fig. 2 DCE-MRI parameter A_{Brix} in relationship to hypoxia gene expression and chemoradiotherapy outcome in cervical cancer. **a** Tumor A_{Brix} map superimposed on axial T2-weighted MR image of two different patients with more hypoxic (left) and less hypoxic (right) tumor. The color scale indicates A_{Brix} values in the range from 0 to ≥ 5.0 .

b Unsupervised clustering of 46 patients based on the expression of 31 hypoxia responsive, A_{Brix} -associated genes (left). Box plot of A_{Brix} for the two patient groups identified by clustering, displaying lower A_{Brix} in cluster with high gene expression (right). **c** Kaplan–Meier survival for progression-free survival of 78 patients with low (below median) and high (above median) A_{Brix} . P value from log-rank test and number of patients are indicated. Reproduced with permission from Halle et al. [46]



[93–95], and it seems that tumor hypoxia can be equally well determined from both modalities. The CT approach is easy to implement due to the linear relationship between attenuation numbers and tracer concentration. DCE-MRI, on the other hand, benefits from the lack of radiation exposure and easy integration with T2 and DW images acquired during the same examination.

Relationship to outcome

A potential clinical relevance of the above findings is demonstrated by a large number of studies showing significant associations between DCE-MRI parameters and clinical outcome (Table 1). In general, low pre-treatment contrast enhancement [96–98], A_{Brix} , K^{trans} , or related

pharmacokinetic parameter [86, 92, 98, 99] has been shown to correlate with poor locoregional control or survival, as illustrated for A_{Brix} in Fig. 2. Most studies include 50 patients or more. Moreover, the fact that similar image parameters are addressed in different patient cohorts and at different institutions, strengthens the conclusions. In addition, Li et al. [100] investigated the relationship of DCE-CT images to outcome in 93 patients, and found that responders had significantly higher values of blood perfusion parameters than non-responders (Table 1).

There are also indications that images acquired during radiotherapy may have prognostic value [101, 102]. In a study of 98 patients, Mayr et al. [101] found that those with persistently low signal enhancement in DCE-MR images acquired before the start of treatment and in the early and mid-phase of the external radiotherapy had the highest risk of treatment failure. In contrast, patients with improved enhancement during therapy, probably reflecting reoxygenation, had favorable outcome, regardless of pre-treatment enhancement. Combining images acquired before and during radiotherapy may, therefore, improve identification of high-risk patients as compared to pre-treatment images. Although promising results, there is, however, no consensus on how to best analyse DCE images to derive the most robust response parameter reflecting hypoxia. Moreover, standardization of the parameters across different MR machines is an unresolved challenge.

Outlook

Other hypoxia PET tracers

For non-cervical cancer, several other hypoxia PET tracers than those mentioned above have been applied clinically [103]. 18F-based nitroimidazoles such as HX4 ([18F]3-fluoro-2-(4-((2-nitro-1H-imidazol-1-yl)methyl)-1H-1,2,3-triazol-1-yl)propan-1-ol) and EF5 ([18F]2-(2-nitro-1H-imidazol-1-yl)-*N*-(2,2,3,3,3-pentafluoropropyl)-acetamide) are available, and both are currently included in clinical studies on patients with cervical cancer (NCT02233387, NCT00978874). However, previous studies provide no evidences that these tracers are superior to the most widely used nitroimidazole, 18F-FMISO [103]. Furthermore, 124Iodine (124I) is a long-lived positron emitter with chemical properties similar to 18F, and may thus allow for imaging at later timepoints after intravenous injection [104]. This could be an advantage for nitroimidazoles, having slow biokinetics. However, e.g., 124I-iodoazomycin arabinoside (124I-IAZA) displayed no favorable characteristics compared to 18F-FAZA in a pre-clinical model [105]. Furthermore, 124I-iodoazomycin galactopyranoside (124I-IAZGP), a

tentative hypoxia marker, showed no significant tumor uptake in patients with colorectal and head and neck cancer [106]. Currently, there seems to be little clinical drive to implement these iodine-based tracers for hypoxia imaging. Thus, there are no indications in the literature of a preferred hypoxia PET tracer or group of tracers that should be tested clinically for cervical cancer.

Combined imaging of flow and metabolism

As noted for DCE imaging, blood flow- or perfusion-based methods may provide surrogate maps of tumor oxygenation. However, the gold standard for assessing blood flow is PET with 15-Oxygen (15O)-labeled water as tracer [107]. It has been argued that regional flow–metabolism mismatch reflects an aggressive tumor phenotype that has adapted to a hypoxic environment [108, 109]. Thus, combined 15O-H₂O and 18F-FDG PET may potentially be used for identifying such tumors. This approach was tested on ten patients with cervical cancer, where substantial regional variations in tumor flow and metabolism were found [109]. However, due to the short half-life of 15O, this approach is not feasible for most cancer centers. Still, studies have shown that ‘first pass’ DCE images after administration of contrast agent reflect tumor blood flow [107, 110]. In addition, different dynamic imaging principles such as MRI, CT, and PET may provide similar estimates of flow-related tumor parameters, as long as proper image acquisition and quantification protocols are followed [93, 94, 111, 112]. Thus, to identify regional flow–metabolism mismatch, one may combine DCE-MRI or DCE-CT with 18F-FDG PET, or perform full dynamic 18F-FDG PET. Using the latter, the patient can be examined in a single scan without the use of additional contrast agents. Hybrid PET/MR or PET/CT scan, where MR or CT is performed as a dynamic scan with contrast agent, may also be attractive. As 18F-FDG is the most widely available PET tracer and DCE methods are straightforward to implement, multiparametric imaging of flow and metabolism should be attractive for further studies addressing tumor hypoxia and aggressiveness in cervical cancer.

Intravoxel incoherent motion (IVIM) DW-MRI

DW-MRI measures the motion of water molecules in tissues. The apparent diffusion coefficient (ADC) of water can be calculated from images with different diffusion weightings [113]. Traditionally, this parameter has been determined by fitting a monoexponential decay curve to plots of signal intensity versus diffusion weighting in terms of ‘*b*’ value. Due to high diffusion coefficient in necrotic tissue, it has been suggested that ADC values can be used

to assess hypoxia [113]. Several studies have indeed reported an association between high pre-treatment ADC and poor outcome in cervical cancer [114, 115]. However, the opposite relationship has also been found [116, 117], probably reflecting an aggressive tumor phenotype with low ADC caused by high cellularity. Moreover, ADC has been shown to correlate with cell density in histological sections [118] and 18F-FDG uptake in PET images [119], but failed to correlate with pO_2 [120] in cervix tumors. A better measure of hypoxia may, however, be achieved by analyzing DW images by the intravoxel incoherent motion (IVIM) model. Here, a biexponential model is employed to separate the blood flow component at b values lower than 200 s/mm^2 , from the diffusion properties of the cellular matrix at b values higher than 300 s/mm^2 [113]. The DWI-based perfusion fraction has been associated with perfusion parameters derived from DCE-MR images (RSI, AUC, A_{Brix} , K^{trans}) in cervical cancer [121, 122], and shown promise as early response indicator during chemoradiotherapy [123]. The IVIM technology, therefore, seems to have a potential in hypoxia imaging of cervix tumors that warrant further investigation.

Combination therapy with hypoxia targeting drug

Combination therapy with radiation and hypoxia targeting drug is as a promising strategy to improve treatment outcome in cervical cancer, and a number of new drugs targeting hypoxia responsive pathways are currently being developed [124]. The optimal drugs for each patient may be decided based on genomic information in a tumor biopsy, which indicates resistance mechanisms at play in the hypoxic tumor. Combining biopsy data with imaging has been proposed as an essential part of a multifactorial decision support system in future radiotherapy planning, presumably leading to more informative decisions and precise selection of high-risk patients [125]. The approach has been evaluated based on a hypoxia gene classifier and DCE-MRI in a pilot study of 64 patients at our institution [45]. Most hypoxic tumors (93%) identified with imaging were detected by the gene classifier. However, the genes classified some additional tumors as hypoxic. The apparent misclassification seemed to be caused by the presence of small hypoxic subpopulations in the regions where the biopsies were taken [126], emphasizing the need for imaging to achieve information from the entire tumor.

The potential of hypoxia imaging in the evaluation of drug effects in clinical trials was elegantly demonstrated in a recent study by Milosevic et al. [8]. They used K^{trans} parametric maps from DCE-MRI to record changes in hypoxia by the angiogenesis inhibitor sorafenib, as illustrated in Fig. 3. The drug was administered for 1 week

prior to radiotherapy to 13 cervical cancer patients to tentatively reduce the amount of hypoxia in the tumors. The imaging data indicated that sorafenib alone increased, rather than decreased, the hypoxic fraction, as confirmed by parallel immunohistochemistry and oxygen electrode measurements. Sorafenib might, therefore, impair the outcome when combined with chemoradiotherapy. Based on this careful monitoring of the tumor hypoxia status, closure of the trial could be decided at an early timepoint.

Radiotherapy dose painting

Radiotherapy dose escalation of resistant tumor regions, or dose painting, is an approach to increase the likelihood of tumor control without irradiating normal tissues to excessively high doses [127]. If hypoxic tumor regions are identified by imaging, the image information can be employed in digital radiotherapy planning systems to deliver escalated radiation doses locally to these regions by advanced radiotherapy techniques, such as volumetric modulated arc therapy or proton therapy [66]. Dose painting of hypoxic cervix tumors has been proposed [7], but has not been clinically implemented to date. This is mainly because local control rate after state-of-the-art combined chemotherapy, external radiotherapy, and brachytherapy is high and around 90% [128]. However, subgroups of patients with advanced and/or hypoxic disease have lower control levels [128], and patients with recurrent disease have few therapy options. By in silico radiotherapy planning, we have shown that external radiotherapy dose escalation of hyperglycolytic regions, identified by 18F-FDG PET, is feasible without increasing the dose to nearby organs [129]. This could lead to higher tumor control probability, with the highest expected gain for stage 3 and 4 tumors. In addition, it could also result in more extensive tumor shrinkage, facilitating less invasive brachytherapy. Although 18F-FDG PET is not a reliable measure of tumor hypoxia, our study shows the feasibility of dose painting in cervix tumors by external radiotherapy. Moreover, if tumor hypoxia is present at brachytherapy, i.e., after external radiotherapy, we have shown the feasibility to target DCE-MRI predicted hypoxic regions with elevated brachytherapy doses [130]. Thus, hypoxia dose painting may be attractive in future trials on cervical cancer, but more work is needed to identify high-risk candidates with persistent tumor hypoxia during treatment.

Conclusion

Tumor hypoxia is a well-known risk factor for patients with cervical cancer, and much work has been done to develop hypoxia imaging procedures and strategies. PET

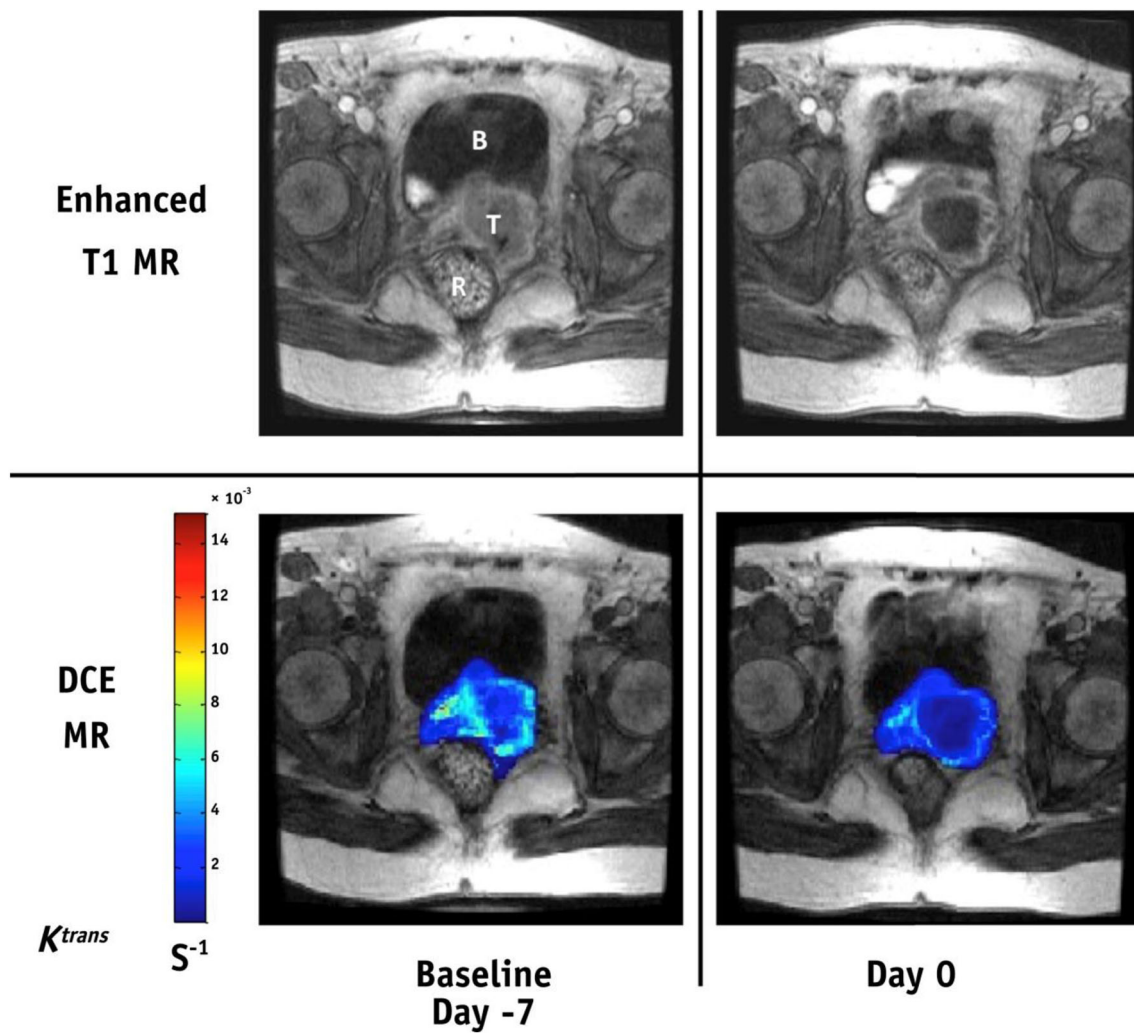


Fig. 3 Changes in cervix tumor hypoxia by the angiogenesis inhibitor sorafenib, assessed by DCE-MRI parameter K^{trans} . Late-phase axial DCE-MR T1 image of pelvis (upper) and the corresponding tumor K^{trans} maps (lower) superimposed on the late-phase

DCE-MR T1 image at baseline before any treatment (day -7 ; left) and after 7 days of sorafenib alone (day 0; right). Note the decrease in K^{trans} after sorafenib treatment. *B* bladder, *R* rectum, *T* tumor. Reproduced with permission from Milosevic et al. [8]

with nitroimidazole tracers is regarded as the gold standard for non-invasive assessment of hypoxia, but the literature on cervical cancer is scarce, with small patient cohorts ($n < 16$), and is, therefore, inconclusive. The lack of PET studies may partly be explained by higher costs and limited availability of scanners and radiotracers. Still, for the few patients investigated with PET, $^{60}\text{Cu}/^{64}\text{Cu}$ -ATSM seems to be the most promising tracer candidate. Furthermore, as T2-weighted MRI has been the diagnostic imaging workhorse in cervical cancer for roughly a decade, implementation of MRI-based sequences, such as BOLD, DCE, and DW, for hypoxia-related studies has been facilitated. This is reflected in the larger body of evidence using surrogate MRI-based measures such as perfusion for hypoxia imaging. Although there is a lack of international protocols for standardized DCE-MR image acquisition and analysis,

results point rather uniformly to the applicability of this modality. Still, contrast-induced nephrogenic toxicity can be a challenge in DCE-MRI. Methods employing endogenous contrast such as BOLD may, therefore, be preferable, although standardization issues prevail, and more work is needed before BOLD imaging is clinically mature. Furthermore, multimodal imaging of flow and metabolism may become attractive, as both hybrid PET/CT and PET/MR scanners can be used for this purpose. Imaging is expected to play a crucial role in future treatment strategies to target hypoxia in cervical cancer, such as drug-radiation combination therapies and radiotherapy dose painting approaches. The ultimate test to decide the optimal imaging method would be a randomized trial comparing hypoxia targeting to the standard treatment with multimodality imaging.

Authors contribution HL: Content planning, Literature Search and Review, Manuscript writing, and Editing. EM: Content planning, Literature Search and Review, Manuscript writing, and Editing.

Compliance with ethical standards

Conflict of interest The authors, Heidi Lyng and Eirik Malinen, have no conflict of interest to declare.

Ethical standards This article does not contain any studies with human or animal subjects performed by the any of the authors.

Open Access This article is distributed under the terms of the Creative Commons Attribution 4.0 International License (<http://creativecommons.org/licenses/by/4.0/>), which permits unrestricted use, distribution, and reproduction in any medium, provided you give appropriate credit to the original author(s) and the source, provide a link to the Creative Commons license, and indicate if changes were made.

References

- Fyles A, Milosevic M, Hedley D, Pintilie M, Levin W, Manchul L, Hill RP (2002) Tumor hypoxia has independent predictor impact only in patients with node-negative cervix cancer. *J Clin Oncol* 20:680–687
- Hockel M, Schlenger K, Aral B, Mitze M, Schaffer U, Vaupel P (1996) Association between tumor hypoxia and malignant progression in advanced cancer of the uterine cervix. *Can Res* 56:4509–4515
- Knocke TH, Weitmann HD, Feldmann HJ, Selzer E, Potter R (1999) Intratumoral $pO(2)$ -measurements as predictive assay in the treatment of carcinoma of the uterine cervix. *Radiother Oncol* 53:99–104
- Lyng H, Sundfor K, Trope C, Rofstad EK (2000) Disease control of uterine cervical cancer: relationships to tumor oxygen tension, vascular density, cell density, and frequency of mitosis and apoptosis measured before treatment and during radiotherapy. *Clin Cancer Res* 6:1104–1112
- Barbera L, Thomas G (2009) Management of early and locally advanced cervical cancer. *Semin Oncol* 36:155–169
- Overgaard J (2007) Hypoxic radiosensitization: adored and ignored. *J Clin Oncol* 25:4066–4074
- Hoskin PJ (2015) Hypoxia dose painting in prostate and cervix cancer. *Acta Oncol* 54:1259–1262
- Milosevic MF, Townsley CA, Chaudary N, Clarke B, Pintilie M, Fan S, Glicksman R, Haider M, Kim S, MacKay H et al (2016) Sorafenib increases tumor hypoxia in cervical cancer patients treated with radiation therapy: results of a Phase 1 clinical study. *Int J Radiat Oncol Biol Phys* 94:111–117
- Lai CH, Lin GG, Yen TC, Liu FY (2014) Molecular imaging in the management of gynecologic malignancies. *Gynecol Oncol* 135:156–162
- Khiewvan B, Torigian DA, Emamzadehfard S, Paydari K, Salavati A, Houshmand S, Shamchi SP, Werner TJ, Aydin A, Roy SG et al (2016) Update of the role of PET/CT and PET/MRI in the management of patients with cervical cancer. *Hell J Nucl Med* 19:254–268
- Nordmark M, Loncaster J, Aquino-Parsons C, Chou SC, West C, Lindegaard JC, Havsteen H, Davidson SE, Raleigh JA, Overgaard J (2006) The prognostic value of pimonidazole and tumor $pO(2)$ in human cervix carcinomas after radiation therapy: an international multi-center study. *Radiother Oncol* 78:S32
- Sundfor K, Lyng H, Trope CG, Rofstad EK (2000) Treatment outcome in advanced squamous cell carcinoma of the uterine cervix: relationships to pretreatment tumor oxygenation and vascularization. *Radiother Oncol* 54:101–107
- Suzuki Y, Nakano T, Ohno T, Kato S, Niibe Y, Morita S, Tsujii H (2006) Oxygenated and reoxygenated tumors show better local control in radiation therapy for cervical cancer. *Int J Gynecol Cancer* 16:306–311
- Wong RKW, Fyles A, Milosevic M, Pintilie M, Hill RP (1997) Heterogeneity of polarographic oxygen tension measurements in cervix cancer: an evaluation of within and between tumor variability, probe position, and track depth. *Int J Radiat Oncol Biol Phys* 39:405–412
- Lyng H, Sundfor K, Rofstad EK (1997) Oxygen tension in human tumours measured with polarographic needle electrodes and its relationship to vascular density, necrosis and hypoxia. *Radiother Oncol* 44:163–169
- Raleigh JA, Chou SC, Bono EL, Thrall DE, Varia MA (2001) Semiquantitative immunohistochemical analysis for hypoxia in human tumors. *Int J Radiat Oncol Biol Phys* 49:569–574
- Michiels C, Tellier C, Feron O (2016) Cycling hypoxia: a key feature of the tumor microenvironment. *Biochim Biophys Acta Rev Cancer* 1866:76–86
- Ellingsen C, Ovrebø KM, Galappathi K, Mathiesen B, Rofstad EK (2012) $pO(2)$ fluctuation pattern and cycling hypoxia in human cervical carcinoma and melanoma xenografts. *Int J Radiat Oncol Biol Phys* 83:1317–1323
- Cairns RA, Hill RP (2004) Acute hypoxia enhances spontaneous lymph node metastasis in an orthotopic murine model of human cervical carcinoma. *Can Res* 64:2054–2061
- Cooper RA, West CML, Logue JP, Davidson SE, Miller A, Roberts S, Statford IJ, Honess DJ, Hunter RD (1999) Changes in oxygenation during radiotherapy in carcinoma of the cervix. *Int J Radiat Oncol Biol Phys* 45:119–126
- Fyles AW, Milosevic M, Pintilie M, Hill RP (1998) Cervix cancer oxygenation measured following external radiation therapy. *Int J Radiat Oncol Biol Phys* 42:751–753
- Lyng H, Sundfor K, Rofstad EK (2000) Changes in tumor oxygen tension during radiotherapy of uterine cervical cancer: relationships to changes in vascular density, cell density, and frequency of mitosis and apoptosis. *Int J Radiat Oncol Biol Phys* 46:935–946
- Sakata KI, Someya M, Nagakura H, Nakata K, Oouchi A, Hareyama M, Satoh M (2006) A clinical study of hypoxia using endogenous hypoxic markers and polarographic oxygen electrodes. *Strahlenther Onkol* 182:511–517
- Lyng H, Sundfor K, Trope C, Rofstad EK (1996) Oxygen tension and vascular density in human cervix carcinoma. *Br J Cancer* 74:1559–1563
- West CML, Cooper RA, Loncaster JA, Wilks DP, Bromley M (2001) Tumor vascularity: a histological measure of angiogenesis and hypoxia. *Can Res* 61:2907–2910
- Hockel S, Schlenger K, Vaupel P, Hockel M (2001) Association between host tissue vascularity and the prognostically relevant tumor vascularity in human cervical cancer. *Int J Oncol* 19:827–832
- Denko NC (2008) Hypoxia, HIF1 and glucose metabolism in the solid tumour. *Nat Rev Cancer* 8:705–713
- Airley RE, Loncaster J, Raleigh JA, Harris AL, Davidson SE, Hunter RD, West CML, Stratford IJ (2003) GLUT-1 and CAIX as intrinsic markers of hypoxia in carcinoma of the cervix: relationship to pimonidazole binding. *Int J Cancer* 104:85–91
- Haugland HK, Vukovic V, Pintilie M, Fyles AW, Milosevic M, Hill RP, Hedley DW (2002) Expression of hypoxia-inducible

- factor-1 alpha in cervical carcinomas: correlation with tumor oxygenation. *Int J Radiat Oncol Biol Phys* 53:854–861
30. Hutchison GJ, Valentine HR, Loncaster JA, Davidson SE, Hunter RD, Roberts SA, Harris AL, Stratford IJ, Price PM, West CML (2004) Hypoxia-inducible factor 1 expression as an intrinsic marker of hypoxia: correlation with tumor oxygen, pimonidazole measurements, and outcome in locally advanced carcinoma of the cervix. *Clin Cancer Res* 10:8405–8412
 31. Jankovic B, Aquino-Parsons C, Raleigh JA, Stanbridge EJ, Durand RE, Banath JP, MacPhail SH, Olive PL (2006) Comparison between pimonidazole binding, oxygen electrode measurements, and expression of endogenous hypoxia markers in cancer of the uterine cervix. *Cytometry Part B Clin Cytometry* 70B:45–55
 32. Loncaster JA, Harris AL, Davidson SE, Logue JP, Hunter RD, Wycoff CC, Pastorek J, Ratcliffe PJ, Stratford IJ, West CML (2001) Carbonic anhydrase (CA IX) expression, a potential new intrinsic marker of hypoxia: correlations with tumor oxygen measurements and prognosis in locally advanced carcinoma of the cervix. *Can Res* 61:6394–6399
 33. Birner P, Schindl M, Obermair A, Plank C, Breitenecker G, Oberhuber G (2000) Overexpression of hypoxia-inducible factor 1 alpha is a marker for an unfavorable prognosis in early-stage invasive cervical cancer. *Can Res* 60:4693–4696
 34. Huang ML, Chen Q, Xiao JP, Yao TT, Bian LJ, Liu CH, Lin ZQ (2014) Overexpression of hypoxia-inducible factor-1 alpha is a predictor of poor prognosis in cervical cancer: a clinicopathologic study and a meta-analysis. *Int J Gynecol Cancer* 24:1054–1064
 35. Liao SY, Darcy KM, Randall LM, Tian CQ, Monk BJ, Burger RA, Fruehauf JP, Peters WA, Stock RJ, Stanbridge EJ (2010) Prognostic relevance of carbonic anhydrase-IX in high-risk, early-stage cervical cancer: a Gynecologic Oncology Group study. *Gynecol Oncol* 116:452–458
 36. Bachtiry B, Schindl M, Potter R, Dreier B, Knocke TH, Hainfellner JA, Horvat R, Birner P (2003) Overexpression of hypoxia-inducible factor 1 alpha indicates diminished response to radiotherapy and unfavorable prognosis in patients receiving radical radiotherapy for cervical cancer. *Clin Cancer Res* 9:2234–2240
 37. Burri P, Djonov V, Aebbersold DM, Lindel K, Studer U, Altermatt HJ, Mazzucchelli L, Greiner RH, Gruber G (2003) Significant correlation of hypoxia-inducible factor-1 alpha with treatment outcome in cervical cancer treated with radical radiotherapy. *Int J Radiat Oncol Biol Phys* 56:494–501
 38. Dellas K, Bache M, Pigorsch SU, Taubert H, Kappler M, Holzzapfel D, Zorn E, Holzhausen HJ, Haensgen G (2008) Prognostic impact of HIF-1 alpha expression in patients with definitive radiotherapy for cervical cancer. *Strahlenther Onkol* 184:169–174
 39. Huang XQ, Liu MM, Sun H, Wang FJ, Xie XX, Chen X, Su J, He YX, Dai YY, Wu HJ, Shen LF (2015) HK2 is a radiation resistant and independent negative prognostic factor for patients with locally advanced cervical squamous cell carcinoma. *Int J Clin Exp Pathol* 8:4054–4063
 40. Iwasaki K, Yabushita H, Ueno T, Wakatsuki A (2015) Role of hypoxia-inducible factor-1 alpha, carbonic anhydrase-IX, glucose transporter-1 and vascular endothelial growth factor associated with lymph node metastasis and recurrence in patients with locally advanced cervical cancer. *Oncol Lett* 10:1970–1978
 41. Kim BW, Cho H, Chung JY, Conway C, Ylaya K, Kim JH, Hewitt SM (2013) Prognostic assessment of hypoxia and metabolic markers in cervical cancer using automated digital image analysis of immunohistochemistry. *J Transl Med* 11(185):1–11
 42. Mayer A, Hockel M, Wree A, Vaupel P (2005) Microregional expression of glucose transporter-1 and oxygenation status: lack of correlation in locally advanced cervical cancers. *Clin Cancer Res* 11:2768–2773
 43. Zhao YJ, Shen LF, Chen X, Qian YJ, Zhou Q, Wang Y, Li K, Liu MM, Zhang S, Huang XQ (2015) High expression of PKM2 as a poor prognosis indicator is associated with radiation resistance in cervical cancer. *Histol Histopathol* 30:1313–1320
 44. Wouters BG, Koritzinsky M (2008) Hypoxia signalling through mTOR and the unfolded protein response in cancer. *Nat Rev Cancer* 8:851–864
 45. Fjeldbo CS, Julin CH, Lando M, Forsberg MF, Aarnes EK, Alsner J, Kristensen GB, Malinen E, Lyng H (2016) Integrative analysis of DCE-MRI and gene expression profiles in construction of a gene classifier for assessment of hypoxia-related risk of chemoradiotherapy failure in cervical cancer. *Clin Cancer Res* 22:4067–4076
 46. Halle C, Andersen E, Lando M, Aarnes EK, Hasvold G, Holden M, Syljuasen RG, Sundfor K, Kristensen GB, Holm R et al (2012) Hypoxia-induced gene expression in chemoradioresistant cervical cancer revealed by dynamic contrast-enhanced MRI. *Can Res* 72:5285–5295
 47. Mujcic H, Nagelkerke A, Rouschop KMA, Chung S, Chaudary N, Span PN, Clarke B, Milosevic M, Sykes J, Hill RP et al (2013) Hypoxic Activation OF the PERK/eIF2 alpha arm of the unfolded protein response promotes metastasis through induction of LAMP3. *Clin Cancer Res* 19:6126–6137
 48. Fleming IN, Manavaki R, Blower PJ, West C, Williams KJ, Harris AL, Domarkas J, Lord S, Baldry C, Gilbert FJ (2015) Imaging tumour hypoxia with positron emission tomography. *Br J Cancer* 112:238–250
 49. Fang SW, Hong MT, Zhang H (2010) Positron emission tomography imaging of tumor hypoxia. *Curr Med Imaging Rev* 6:8–16
 50. Imam SK (2010) Review of positron emission tomography tracers for imaging of tumor hypoxia. *Cancer Biother Radiopharm* 25:365–374
 51. Varghese AJ, Whitmore GF (1980) Binding to cellular macromolecules as a possible mechanism for the cyto-toxicity of misonidazole. *Can Res* 40:2165–2169
 52. Lee ST, Scott AM (2007) Hypoxia positron emission tomography imaging with F-18-fluoromisonidazole. *Semin Nucl Med* 37:451–461
 53. Lewis JS, Laforest R, Dehdashti F, Grigsby PW, Welch MJ, Siegel BA (2008) An imaging comparison of Cu-64-ATSM and Cu-60-ATSM in cancer of the uterine cervix. *J Nucl Med* 49:1177–1182
 54. Vavere AL, Lewis JS (2007) Cu-ATSM: a radiopharmaceutical for the PET imaging of hypoxia. *Dalton Trans* 43:4893–4902
 55. Holland JP, Lewis JS, Dehdashti F (2009) Assessing tumor hypoxia by positron emission tomography with Cu-ATSM. *Q J Nucl Med Mol Imaging* 53:193–200
 56. Koh WJ, Rasey JS, Evans ML, Grierson JR, Lewellen TK, Graham MM, Krohn KA, Griffin TW (1992) Imaging of hypoxia in human tumors with [F-18] fluoromisonidazole. *Int J Radiat Oncol Biol Phys* 22:199–212
 57. Pinker K, Andrzejewski P, Baltzer P, Polanec SH, Sturdza A, Georg D, Helbich TH, Karanikas G, Grimm C, Polterauer S et al (2016) Multiparametric [F-18]fluorodeoxyglucose/[F-18]fluoromisonidazole positron emission tomography/magnetic resonance imaging of locally advanced cervical cancer for the non-invasive detection of tumor heterogeneity: a pilot study. *PLoS One* 11(5):e0155333
 58. Busk M, Horsman MR, Jakobsen S, Keiding S, van der Kogel AJ, Bussink J, Overgaard J (2008) Imaging hypoxia in xenografted and murine tumors with F-18-fluoroazomycin arabinoside: a comparative study involving micropet, autoradiography, Po-2-polarography, and fluorescence microscopy. *Int J Radiat Oncol Biol Phys* 70:1202–1212

59. Schuetz M, Schmid MP, Potter R, Kommata S, Georg D, Lukic D, Dudczak R, Kletter K, Dimopoulos J, Karanikas G, Bachtary B (2010) Evaluating repetitive F-18-fluorazomycin-araboside ((18)FAZA) PET in the setting of MRI guided adaptive radiotherapy in cervical cancer. *Acta Oncol* 49:941–947
60. Vercellino L, Groheux D, Thoury A, Delord M, Schlageter MH, Delpech Y, Barre E, Baruch-Hennequin V, Tylski P, Homyrda L et al (2012) Hypoxia imaging of uterine cervix carcinoma with F-18-FETNIM PET/CT. *Clin Nucl Med* 37:1065–1068
61. Le QT, Sutphin PD, Raychaudhuri S, Yu SCT, Terris DJ, Lin HS, Lum B, Pinto HA, Koong AC, Giaccia AJ (2003) Identification of osteopontin as a prognostic plasma marker for head and neck squamous cell carcinomas. *Clin Cancer Res* 9:59–67
62. Dehdashti F, Grigsby PW, Lewis JS, Laforest R, Siegel BA, Welch MJ (2008) Assessing tumor hypoxia in cervical cancer by PET with Cu-60-labeled diacetyl-bis(N-4-methylthiosemicarbazone). *J Nucl Med* 49:201–205
63. Dehdashti F, Grigsby PW, Mintun MA, Lewis JS, Siegel BA, Welch MJ (2003) Assessing tumor hypoxia in cervical cancer by positron emission tomography with Cu-60-ATSM: relationship to therapeutic response—a preliminary report. *Int J Radiat Oncol Biol Phys* 55:1233–1238
64. Grigsby PW, Malyapa RS, Higashikubo R, Schwarz JK, Welch MJ, Huettner PC, Dehdashti F (2007) Comparison of molecular markers of hypoxia and imaging with Cu-60-ATSM in cancer of the uterine cervix. *Mol Imag Biol* 9:278–283
65. Dence CS, Ponde DE, Welch MJ, Lewis JS (2008) Autoradiographic and small-animal PET comparisons between F-18-FMISO, F-18-FDG, F-18-FLT and the hypoxic selective Cu-64-ATSM in a rodent model of cancer. *Nucl Med Biol* 35:713–720
66. O'Donoghue JA, Zanzonico P, Pugachev A, Wen BX, Smith-Jones P, Cai SD, Burnazi E, Finn RD, Burgman P, Ruan S et al (2005) Assessment of regional tumor hypoxia using F-18-fluoromisonidazole and Cu-64(II)-diacetyl-bis(N-4-methylthiosemicarbazone) positron emission tomography: comparative study featuring microPET imaging, *Po-2* probe measurement, autoradiography, and fluorescent microscopy in the R3327-AT and FaDu rat tumor models. *Int J Radiat Oncol Biol Phys* 61:1493–1502
67. Yuan H, Schroeder T, Bowsher JE, Hedlund LW, Wong T, Dewhurst MW (2006) Intertumoral differences in hypoxia selectivity of the PET imaging agent Cu-64(II)-diacetyl-bis(N-4-methylthiosemicarbazone). *J Nucl Med* 47:989–998
68. Grigsby PW (2008) The prognostic value of PET and PET/CT in cervical cancer. *Cancer Imaging* 8:146–155
69. Zimny M, Gagel B, DiMartino E, Hamacher K, Coenen HH, Westhofen M, Eble M, Buell U, Reinartz P (2006) FDG—a marker of tumour hypoxia? A comparison with [F-18] fluoromisonidazole and *pO(2)*-polarography in metastatic head and neck cancer. *Eur J Nucl Med Mol Imaging* 33:1426–1431
70. Busk M, Horsman MR, Kristjansen PEG, van der Kogel AJ, Bussink J, Overgaard J (2008) Aerobic glycolysis in cancers: implications for the usability of oxygen-responsive genes and fluorodeoxyglucose-PET as markers of tissue hypoxia. *Int J Cancer* 122:2726–2734
71. Christian N, Deheneff S, Bol A, De Bast M, Labar D, Lee JA, Gregoire V (2010) Is F-18-FDG a surrogate tracer to measure tumor hypoxia? Comparison with the hypoxic tracer C-14-EF3 in animal tumor models. *Radiother Oncol* 97:183–188
72. Dierckx RA, de Wiele CV (2008) FDG uptake, a surrogate of tumour hypoxia? *Eur J Nucl Med Mol Imaging* 35:1544–1549
73. Horsman MR, Mortensen LS, Petersen JB, Busk M, Overgaard J (2012) Imaging hypoxia to improve radiotherapy outcome. *Nat Rev Clin Oncol* 9:674–687
74. Cheng YX, Chen GT, Hong L, Zhou LM, Hu M, Li BS, Huang JL, Xia LB, Li CL (2013) How does hypoxia inducible factor-1 alpha participate in enhancing the glycolysis activity in cervical cancer? *Ann Diagn Pathol* 17:305–311
75. Park SI, Suh DS, Kim SJ, Choi KU, Yoon MS (2013) Correlation between biological marker expression and F-18-fluorodeoxyglucose uptake in cervical cancer measured by position emission tomography. *Onkologie* 36:169–174
76. Price JM, Robinson SP, Koh DM (2013) Imaging hypoxia in tumours with advanced MRI. *Q J Nucl Med Mol Imaging* 57:257–270
77. Hallac RR, Ding Y, Yuan Q, McColl RW, Lea J, Sims RD, Weatherall PT, Mason RP (2012) Oxygenation in cervical cancer and normal uterine cervix assessed using blood oxygenation level-dependent (BOLD) MRI at 3T. *NMR Biomed* 25:1321–1330
78. O'Connor JPB, Naish JH, Parker GJM, Waterton JC, Watson Y, Jayson GC, Buonaccorsi GA, Cheung S, Buckley DL, McGrath DM et al (2009) Preliminary study of oxygen-enhanced longitudinal relaxation in MRI: a potential novel biomarker of oxygenation changes in solid tumors. *Int J Radiat Oncol Biol Phys* 75:1209–1215
79. Ciris PA, Balasubramanian M, Damato AL, Seethamraju RT, Tempany-Afdhal CM, Mulkern RV, Viswanathan AN (2016) Characterizing gradient echo signal decays in gynecologic cancers at 3T using a Gaussian augmentation of the monoexponential (GAME) model. *J Magn Reson Imaging* 44:1020–1030
80. Kim CK, Park SY, Park BK, Park W, Huh SJ (2014) Blood oxygenation level-dependent MR imaging as a predictor of therapeutic response to concurrent chemoradiotherapy in cervical cancer: a preliminary experience. *Eur Radiol* 24:1514–1520
81. Choi SH, Kim CK, Park JJ, Park BK (2016) Assessment of early therapeutic changes to concurrent chemoradiotherapy in uterine cervical cancer using blood oxygenation level-dependent magnetic resonance imaging. *J Comput Assist Tomogr* 40:730–734
82. Li XS, Fan HX, Fang H, Song YL, Zhou CW (2015) Value of $R2^*$ obtained from $T2^*$ -weighted imaging in predicting the prognosis of advanced cervical squamous carcinoma treated with concurrent chemoradiotherapy. *J Magn Reson Imaging* 42:681–688
83. Mahajan A, Engineer R, Chopra S, Mahanshetty U, Juvekar SL, Shrivastava SK, Desekar N, Thakura MH (2016) Role of 3T multiparametric-MRI with BOLD hypoxia imaging for diagnosis and post therapy response evaluation of postoperative recurrent cervical cancers. *Eur J Radiol Open* 3:22–30
84. Hasebroock KM, Serkova NJ (2009) Toxicity of MRI and CT contrast agents. *Expert Opin Drug Metab Toxicol* 5:403–416
85. Zahra MA, Hollingsworth KG, Sala E, Lomas DJ, Tan LT (2007) Dynamic contrast-enhanced MRI as a predictor of tumour response to radiotherapy. *Lancet Oncol* 8:63–74
86. Lancaster JA, Carrington BM, Sykes JR, Jones AP, Todd SM, Cooper R, Buckley DL, Davidson SE, Logue JP, Hunter RD, West CML (2002) Prediction of radiotherapy outcome using dynamic contrast enhanced MRI of carcinoma of the cervix. *Int J Radiat Oncol Biol Phys* 54:759–767
87. Lyng H, Vorren AO, Sundfor K, Taksdal I, Lien HH, Kaalhus A, Rofstad EK (2001) Assessment of tumor oxygenation in human cervical carcinoma by use of dynamic Gd-DTPA-enhanced MR imaging. *J Magn Reson Imaging* 14:750–756
88. Haider MA, Milosevic M, Fyles A, Sitartchouk I, Yeung I, Henderson E, Lockwood G, Lee TY, Roberts TPL (2005) Assessment of the tumor microenvironment in cervix cancer using dynamic contrast enhanced CT, interstitial fluid pressure and oxygen measurements. *Int J Radiat Oncol Biol Phys* 62:1100–1107
89. Hawighorst H, Knapstein PG, Knopp MV, Weikel W, Brix G, Zuna I, Schonberg SO, Essig M, Vaupel P, van Kaick G (1998)

- Uterine cervical carcinoma: comparison of standard and pharmacokinetic analysis of time-intensity curves for assessment of tumor angiogenesis and patient survival. *Can Res* 58:3598–3602
90. Tofts PS (1997) Modeling tracer kinetics in dynamic Gd-DTPA MR imaging. *J Magn Reson Imaging* 7:91–101
 91. Tofts PS, Brix G, Buckley DL, Evelhoch JL, Henderson E, Knopp M, Larsson HBW, Lee TY, Mayr NA, Parker GJM et al (1999) Estimating kinetic parameters from dynamic contrast-enhanced T(1)-weighted MRI of a diffusible tracer: standardized quantities and symbols. *J Magn Reson Imaging* 10:223–232
 92. Andersen EKF, Hole KH, Lund KV, Sundfor K, Kristensen GB, Lyng HD, Malinen E (2013) Pharmacokinetic parameters derived from dynamic contrast enhanced MRI of cervical cancers predict chemoradiotherapy outcome. *Radiother Oncol* 107:117–122
 93. Kallehauge J, Nielsen T, Haack S, Peters DA, Mohamed S, Fokdal L, Lindegaard JC, Hansen DC, Rasmussen F, Tanderup K, Pedersen EM (2013) Voxelwise comparison of perfusion parameters estimated using dynamic contrast enhanced (DCE) computed tomography and DCE-magnetic resonance imaging in locally advanced cervical cancer. *Acta Oncol* 52:1360–1368
 94. Kim SM, Haider MA, Milosevic M, Yeung IWT (2013) A comparison of dynamic contrast-enhanced CT and MR imaging-derived measurements in patients with cervical cancer. *Clin Physiol Funct Imaging* 33:150–161
 95. Yang C, Stadler WM, Karczmar GS, Milosevic M, Yeung I, Haider MA (2010) Comparison of quantitative parameters in cervix cancer measured by dynamic contrast-enhanced MRI and CT. *Magn Reson Med* 63:1601–1609
 96. Andersen EKF, Hole KH, Lund KV, Sundfor K, Kristensen GB, Lyng H, Malinen E (2012) Dynamic contrast-enhanced MRI of cervical cancers: temporal percentile screening of contrast enhancement identifies parameters for prediction of chemoradioresistance. *Int J Radiat Oncol Biol Phys* 82:E485–E492
 97. Lund KV, Simonsen TG, Hompland T, Kristensen GB, Rofstad EK (2015) Short-term pretreatment DCE-MRI in prediction of outcome in locally advanced cervical cancer. *Radiother Oncol* 115:379–385
 98. Zahra MA, Tan LT, Priest AN, Graves MJ, Arends M, Crawford RAF, Brenton JD, Lomas DJ, Sala E (2009) Semicquantitative and quantitative dynamic contrast-enhanced magnetic resonance imaging measurements predict radiation response in cervix cancer. *Int J Radiat Oncol Biol Phys* 74:766–773
 99. Hawighorst H, Weikel W, Knapstein PG, Knopp MV, Zuna I, Schonberg SO, Vaupel P, van Kaick G (1998) Angiogenic activity of cervical carcinoma: assessment by functional magnetic resonance imaging-based parameters and a histomorphological approach in correlation with disease outcome. *Clin Cancer Res* 4:2305–2312
 100. Li XS, Fan HX, Zhu HX, Song YL, Zhou CW (2012) The value of perfusion CT in predicting the short-term response to synchronous radiochemotherapy for cervical squamous cancer. *Eur Radiol* 22:617–624
 101. Mayr NA, Wang JZ, Zhang DQ, Grecula JC, Lo SS, Jaroura D, Montebello J, Zhang HL, Li KL, Lu LC et al (2010) Longitudinal changes in tumor perfusion pattern during the radiation therapy course and its clinical impact in cervical cancer. *Int J Radiat Oncol Biol Phys* 77:502–508
 102. Yuh WTC, Mayr NA, Jarjoura D, Wu D, Grecula JC, Lo SS, Edwards SM, Magnotta VA, Sammet S, Zhang H et al (2009) Predicting control of primary tumor and survival by DCE MRI during early therapy in cervical cancer. *Invest Radiol* 44:343–350
 103. Challapalli A, Carroll L, Aboagye EO (2017) Molecular mechanisms of hypoxia in cancer. *Clin Transl Imaging* 5:225–253
 104. Cascini GL, Asabella AN, Notaristefano A, Restuccia A, Ferrari C, Rubini D, Altini C, Rubini G (2014) Iodine: a longer-life positron emitter isotope—new opportunities in molecular imaging. *Biomed Res Int* 2014:672094. doi:10.1155/2014/672094
 105. Reischl G, Dorow DS, Cullinane C, Katsifis A, Roselt P, Binns D, Hicks RJ (2007) Imaging of tumor hypoxia with [I-124] IAZA in comparison with [F-18] FMISO and [F-18]FAZA—first small animal PET results. *J Pharm Pharm Sci* 10:203–211
 106. O'Donoghue JA, Guillem JG, Schoder H, Lee NY, Divgi CR, Ruby JA, Humm JL, Lee-Kong SA, Burnazi EM, Cai SD et al (2013) Pilot study of PET imaging of I-124-iodoazomycin galactopyranoside (IAZGP), a putative hypoxia imaging agent, in patients with colorectal cancer and head and neck cancer. *Ejnmri Res* 3(42):1–10
 107. Mullani NA, Herbst RS, O'Neil RG, Gould KL, Barron BJ, Abbruzzese JL (2008) Tumor blood flow measured by PET dynamic imaging of first-pass F-18-FDG uptake: a comparison with O-15-labeled water-measured blood flow. *J Nucl Med* 49:517–523
 108. An YS, Kang DK, Jung YS, Han S, Kim TH (2015) Tumor metabolism and perfusion ratio assessed by 18F-FDG PET/CT and DCE-MRI in breast cancer patients: correlation with tumor subtype and histologic prognostic factors. *Eur J Radiol* 84:1365–1370
 109. Apostolova I, Hofheinz F, Buchert R, Steffen IG, Michel R, Rosner C, Prasad V, Kohler C, Derlin T, Brenner W, Marnitz S (2014) Combined measurement of tumor perfusion and glucose metabolism for improved tumor characterization in advanced cervical carcinoma A PET/CT pilot study using [O-15]water and [F-18]fluorodeoxyglucose. *Strahlenther Onkol* 190:575–581
 110. De Langen AJ, van den Boogaart VEM, Marcus JT, Lubberink M (2008) Use of (H₂O)-O-15-PET and DCE-MRI to measure tumor blood flow. *Oncologist* 13:631–644
 111. Malinen E, Rodal J, Knudtsen IS, Sovik A, Skogmo HK (2011) Spatiotemporal analysis of tumor uptake patterns in dynamic (18)FDG-PET and dynamic contrast enhanced CT. *Acta Oncol* 50:873–882
 112. Yang DJ, Kim EE, Inoue T (2006) Targeted molecular imaging in oncology. *Ann Nucl Med* 20:1–11
 113. Thoeny HC, Ross BD (2010) Predicting and monitoring cancer treatment response with diffusion-weighted MRI. *J Magn Reson Imaging* 32:2–16
 114. Heo SH, Shin SS, Kim JW, Lim HS, Jeong YY, Kang WD, Kim SM, Kang HK (2013) Pre-treatment diffusion-weighted MR imaging for predicting tumor recurrence in uterine cervical cancer treated with concurrent chemoradiation: value of histogram analysis of apparent diffusion coefficients. *Korean J Radiol* 14:616–625
 115. Marconi DG, Fregnani JHTG, Rossini RR, Netto AKB, Lucchesi FR, Tsunoda AT, Kamrava M (2016) Pre-treatment MRI minimum apparent diffusion coefficient value is a potential prognostic imaging biomarker in cervical cancer patients treated with definitive chemoradiation. *BMC Cancer* 16(556):1–9
 116. Gladwish A, Milosevic M, Fyles A, Xie J, Halankar J, Metser U, Jiang HY, Becker N, Levin W, Manchul L et al (2016) Association of apparent diffusion coefficient with disease recurrence in patients with locally advanced cervical cancer treated with radical chemotherapy and radiation therapy. *Radiology* 279:158–166
 117. Onal C, Erbay G, Guler OC (2016) Treatment response evaluation using the mean apparent diffusion coefficient in cervical cancer patients treated with definitive chemoradiotherapy. *J Magn Reson Imaging* 44:1010–1019
 118. Liu Y, Bai RJ, Sun HR, Liu HD, Wang DH (2009) Diffusion-weighted magnetic resonance imaging of uterine cervical cancer. *J Comput Assist Tomogr* 33:858–862

119. Nakamura K, Joja I, Kodama J, Hongo A, Hiramatsu Y (2012) Measurement of SUVmax plus ADCmin of the primary tumour is a predictor of prognosis in patients with cervical cancer. *Eur J Nucl Med Mol Imaging* 39:283–290
120. McVeigh PZ, Syed AM, Milosevic M, Fyles A, Haider MA (2008) Diffusion-weighted MRI in cervical cancer. *Eur Radiol* 18:1058–1064
121. Lee EYP, Hui ESK, Chan KKL, Tse KY, Kwong WK, Chang TY, Chan Q, Khong PL (2015) Relationship between intravoxel incoherent motion diffusion-weighted MRI and dynamic contrast-enhanced MRI in tissue perfusion of cervical cancers. *J Magn Reson Imaging* 42:454–459
122. Zhou Y, Liu JY, Liu CR, Jia J, Li N, Xie LZ, Zhou ZY, Zhang ZH, Zheng DD, He W et al (2016) Intravoxel incoherent motion diffusion weighted MRI of cervical cancer—correlated with tumor differentiation and perfusion. *Magn Reson Imaging* 34:1050–1056
123. Zhu L, Zhu LJ, Shi H, Wang HH, Yan J, Liu BR, Chen WB, He J, Zhou ZY, Yang XF, Liu T (2016) Evaluating early response of cervical cancer under concurrent chemo-radiotherapy by intravoxel incoherent motion MR imaging. *BMC Cancer* 16(79):1–8
124. Rey S, Schito L, Koritzinsky M, Wouters BG (2017) Molecular targeting of hypoxia in radiotherapy. *Adv Drug Deliv Rev* 109:45–62
125. Lambin P, van Stiphout RGPM, Starmans MHW, Rios-Velazquez E, Nalbantov G, Aerts HJWL, Roelofs E, van Elmpt W, Boutros PC, Granone P et al (2013) Predicting outcomes in radiation oncology-multifactorial decision support systems. *Nat Rev Clin Oncol* 10:27–40
126. Fjeldbo CS, Aarnes EK, Malinen E, Kristensen GB, Lyng H (2016) Identification and Validation of Reference Genes for RT-qPCR Studies of Hypoxia in Squamous Cervical Cancer Patients. *PLoS One* 11(5):e0156259
127. Sovik A, Malinen E, Olsen DR (2009) Strategies for biologic image-guided dose escalation: a review. *Int J Radiat Oncol Biol Phys* 73:650–658
128. Sturdza A, Potter R, Fokdal LU, Haie-Meder C, Tan LT, Mazon R, Petric P, Segedin B, Jurgenliemk-Schulz IM, Nomden C et al (2016) Image guided brachytherapy in locally advanced cervical cancer: improved pelvic control and survival in RetroEMBRACE, a multicenter cohort study. *Radiother Oncol* 120:428–433
129. Xu HQ, Li B, Yu WJ, Wang H, Zhao XF, Yao YC, Huang DK (2013) Correlation between F-18-FDG uptake and the expression of glucose transporter-1 and hypoxia-inducible factor-1 in transplanted VX2 tumors. *Nucl Med Commun* 34:953–958
130. Li A, Andersen E, Lervåg C, Julin CH, Lyng H, Hellebust TP, Malinen E (2017) Dynamic contrast enhanced magnetic resonance imaging for hypoxia mapping and potential for brachytherapy targeting. *Phys Imaging Radiat Oncol* 2:1–6